Kinetic study of an autocatalytic reaction: nitrosation of formamidine disulfide†

Vitor Francisco,[a] Luis Garcia-Rio,*[a] José António Moreira[ab] and Geoffrey Stedman[a]

Received (in Durham, UK) 26th June 2008, Accepted 20th August 2008
First published as an Advance Article on the web 14th October 2008
DOI: 10.1039/b810761k

The reaction kinetics for the acid nitrosation of formamidine disulfide (FDS) show an autocatalytic behavior that arises from the fact that the thiocyanate ion formed as a product acts as a powerful catalyst for the nitrosation reaction. In the presence of added nucleophiles the suppression of the autocatalytic route results from competition for the nitrous acid between the added halides and the thiocyanate anion, which is formed as a reaction product. Analysis of the kinetic data enabled extraction of the bimolecular rate constants, $k_{NO^+} = (3.2 \pm 1.8) \times 10^{10}$ M^{-1} s^{-1}; $k_{NOSCN} = (2.1 \pm 0.2) \times 10^5$ M^{-1} s^{-1}; $k_{NOBr} = (9.4 \pm 0.2) \times 10^6$ M^{-1} s^1 and $k_{NOCl} = (4.0 \pm 0.2) \times 10^7$ M^{-1} s^{-1}, for the pathways catalyzed by SCN^-, Br^- and Cl^-, respectively. Kinetic results are consistent with the attack on the nitrosating agent as the rate limiting step, *i.e.*, the nitrosation of FDS behaves in a similar manner to the nitrosation of an amine. Rather different behavior is found for other substrates with an imino moiety adjacent to an amino nitrogen, such as the guanidines, which react by a mechanism in which the rate limiting step is the reorganization of the nitrosated substrate.

Introduction

Nitrosation reactions have important industrial,[1] environmental[2] and physiological[3] relevance and are involved in the production of highly carcinogenic compounds such as nitrosamines.[4] Increasing attention is being paid to the chemistry of nitrosamines owing to the toxicity[5] and carcinogenic,[6] mutagenic,[7] and teratogenic[8] properties of these compounds. In more recent times, since the discovery of the amazing biological properties of nitric oxide there has been a large interest in the chemistry of S-nitrosothiols, these can act as possible vasodilators, anti-platelet aggregation agents *etc.*[9]

In this paper we report the kinetics for the nitrosation of formamidine disulfide (FDS). Formamidine disulfide is a dimeric species that is produced from the, rather complex, oxidation of thiourea.[10,11] Formamidine disulfide also provides a convenient method to prepare monosubstituted guanidines,[12] and is also used as an active oxidant in gold leaching systems.[13] Formamidine disulfide also has an established role in biochemistry as a potent inhibitor of the enzyme amidinase transferase[14] and of D-amino acid oxidaze,[15] with the disulfide character being a requisite for the inhibitory action since the enzyme inhibition results from the sulfhydryl disulfide exchange, blocking the use of the enzyme SH function.

In the absence of added nucleophilic species, nitrous acid produces two nitrosating agents: the nitrosyl ion (NO^+) and dinitrogen trioxide (N_2O_3).[16] NO^+ is formed by the protonation and subsequent dehydration of nitrous acid, while N_2O_3 is formed under mildly acidic conditions (Scheme 1). The nitrosyl ion is highly reactive and in most cases the rates of reactions involving this species are diffusion controlled.[17] However, the observed rate constants are small and easily measured due to the low concentration of the nitrosyl ion in the acidic medium ($K_{NO} = 3 \times 10^{-7}$ M^{-1}).[16,18] The exact nature of the NO^+ ion is still a matter of debate, especially at high acidity values where the form $HNOO^+H$[9] also occurs. Nevertheless, this difference is rather unimportant in the present study since both proposed nitrosating agents would be kinetically equivalent.

A common feature of many nitrosation reactions is the ability of halide ions, the thiocyanate ion and other nucleophiles to act as catalysts in acidic solution.[19] This is due to the equilibrium displacement towards the nitrosating agent NOX, when compared with the equilibrium constant of NO^+ formation ($K_{NOX} = 1.1 \times 10^{-3}$, 5.1×10^{-2} and 30 M^{-2} for X = Cl, Br and SCN, respectively).[20–22] The rate constants for the nitroso group transfer from NOX follow the order NOCl > NOBr > NOSCN,[23–27] demonstrating that the catalytic effect is due to the thermodynamics of the formation of the nitrosating agent.

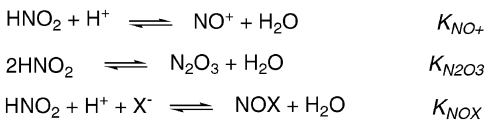

Scheme 1

[a] *Departamento de Química Física, Universidad de Santiago de Compostela, 15782 Santiago de Compostela, Spain*
[b] *CIQA Departamento de Química, Bioquímica e Farmácia, FCT, Universidade do Algarve, Campus de Gambelas, 8005-139 Faro, Portugal. E-mail: qflgr3cn@usc.es*

† Electronic supplementary information (ESI) available: Derivation of rate equations. See DOI: 10.1039/b810761k

In the latter years of the 19th century, Storch[28] showed that treatment of thiourea with nitrous acid led to the formation of a weak base (eqn (1)). Subsequently, Werner[29,30] was able to observe the formation of a transient red intermediate, identified by Stedman and co-workers as $(NH_2)_2CSNO^+$,[31–33] and to isolate the product formamidine disulfide in the form of the salt $(NH_2)_2CSSC(NH_2)_2{}^{2+}2X^-$.

$$2H^+ + 2HNO_2 + 2(NH_2)_2CS \rightarrow (NH_2)_2CSSC(NH_2)_2{}^{2+} + 2NO + 2H_2O \quad (1)$$

Werner found that an excess of nitrous acid gave a further reaction, which led to the destruction of the formamidine disulfide.

$$3(NH_2)_2CSSC(NH_2)_2{}^{2+} + 6HNO_2 \rightarrow 6N_2 + 5HNCS + H_2SO_4 + HCN + 6H^+ \quad (2)$$

The stability of formamidine disulfide in aqueous solution has also been studied[34] and pK_a values of 5.49 and 7.66 have been measured. The formamidine disulfide decomposition (eqn (3)) involves one reactive tautomer of the doubly charged cation $(HN{=})(NH_3{}^+)CSSC^+(NH_2)_2$, which is attacked by H_2O and a singly charged cation, resulting from the deprotonation of the diprotonated formamidine disulfide, which reacts through two parallel pathways involving OH^- and H_2O as attacking bases.

$$(NH_2)_2CSSC(NH_2)_2{}^{2+} + 2OH^- \rightarrow (NH_2)_2CS + S + NH_2CN + 2H_2O \quad (3)$$

In the present work we focused our attention on reaction (2) in the knowledge that complex behavior should be expected. Nitrosation of FDS involves the formation of the thiocyanate ion, which reacts with HNO_2 to yield the nitrosating agent NOSCN. As a result, an autocatalytic reaction will be observed.

Experimental

Materials

Formamidine disulfide dihydrochloride ($FDSH_2{}^{2+}2Cl^-$) was initially synthesized following Werner's method.[29] The results are perfectly compatible with those obtained using the formamidine disulfide dihydrochloride (97.0%) supplied by Aldrich. Stock solutions of $FDSH_2{}^{2+}2Cl^-$ were kept in excess perchloric acid to minimize decomposition, and fresh solutions were made up daily from the solid salt. All other chemicals were obtained from Aldrich and used without further purification. Cyanhydric acid (HCN) is formed in this reaction, special precautions must be taken when the reaction is carried out at higher concentrations of FDS.

Kinetic methods

Reaction rates were monitored spectrophotometrically at 370 nm, using a Cary 50 spectrophotometer at 25.0 °C. The ionic strength was kept constant (I = 1.00 M) by adding the appropriate amount of $NaClO_4$. The reactions were performed by mixing in the quartz cell the appropriate amounts of $FDSH_2Cl_2$, $HClO_4$, $NaNO_2$, NaSCN or, alternatively, NaCl and NaBr solutions. $NaNO_2$ was always added at the end in order to trigger the reaction. Kinetic analysis of absorbance *vs.* time data was performed by fitting the experimental data to the appropriate equation using the commercial software package Grafit.[35]

Results and discussion

1. Reaction in the absence of added halide ions

Nitrosation of $FDSH_2{}^{2+}$ involves the formation of the thiocyanate ion, which reacts with HNO_2 to yield the nitrosating agent NOSCN. As a result, an autocatalytic reaction was observed. Further evidence concerning the autocatalytic reaction was obtained by studying the nitrosation reaction in the presence of a large concentration of SCN^- (see below). In the experiments carried out at higher FDS concentration the presence of gas bubbles is observed, this is due to the formation of N_2 as reaction product The rate of the nitrosation process is given by the following equation, where FDS_r represents the reactive form of FDS.

$$r = k_{NO^+}[NO^+][FDS_r] + k_{NOSCN}[FDS_r][NOSCN] \quad (4)$$

We must account for the following equilibria (Scheme 2):

All experiments were carried out in the pH range 0–2, so we expect that the reactive form of FDS should be the monoprotonated ($FDSH^+$). According to this situation, eqn (4) should be rewritten as:

$$r = k_{NO^+}K_{NO^+}K_a{}^I[HNO_2][FDSH_2{}^{2+}] + k_{NOSCN}K_{NOSCN}K_a{}^I[FDSH_2{}^{2+}][SCN^-][HNO_2] \quad (5)$$

In all cases $[FDSH_2{}^{2+}] \gg [HNO_2]$, so we can consider $[FDSH_2{}^{2+}] \cong [FDSH_2{}^{2+}]_0$, and as $[SCN^-]$ at each instant is proportional to the consumed HNO_2, $[SCN^-] = 5/6([HNO_2]_0 - [HNO_2])$, the rate eqn (5) can be simplified to:

$$r = k_1[HNO_2] + 5/6k_2[HNO_2]([HNO_2]_0 - [HNO_2]) \quad (6)$$

Where $k_1 = k_{NO^+}K_{NO^+}K_a{}^I[FDSH_2{}^{2+}]_0$ and $k_2 = k_{NOSCN}K_{NOSCN}K_a{}^I[FDSH_2{}^{2+}]_0$.

$$r = d[HNO_2]/dt = (k_1 + 5/6k_2[HNO_2]_0)[HNO_2] - 5/6k_2[HNO_2]^2 \quad (7)$$

Considering: $k_3 = k_1 + 5/6k_2[HNO_2]_0$, then:

$$-\int_{[HNO_2]_0}^{[HNO_2]} \frac{d[HNO_2]}{k_3[HNO_2] - 5/6k_2[HNO_2]^2} = \int_0^t dt \quad (8)$$

Integrating the former equation we obtain:

$$[HNO_2] = \frac{k_3[HNO_2]_0}{(k_3 - 5/6k_2[HNO_2]_0)e^{k_3 t} + 5/6k_2[HNO_2]_0} \quad (9)$$

The reaction kinetics were studied at 370 nm by following the disappearance of HNO_2. Considering A_t, A_∞ and A_0 as the measured absorbances at time t, at the end of the reaction and

$HNO_2 + H^+ \rightleftharpoons NO^+ + H_2O$ K_{NO+}
$HNO_2 + H^+ + SCN^- \rightleftharpoons NOSCN + H_2O$ K_{NOSCN}
$FDSH_2{}^{2+} \rightleftharpoons FDSH^+ + H^+$ $K_a{}^I$
$FDSH^+ \rightleftharpoons FDS + H^+$ $K_a{}^{II}$

Scheme 2

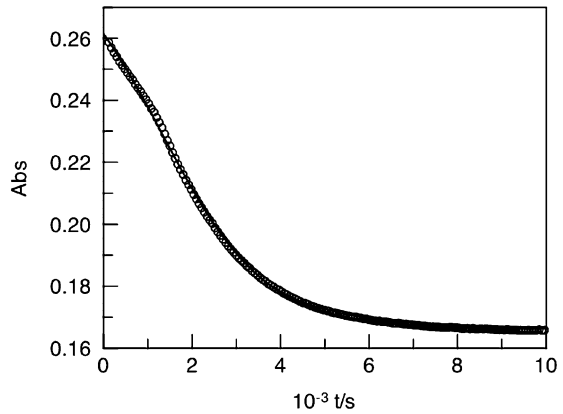

Fig. 1 Absorbance *vs.* time plot for the reaction of HNO_2 with $FDSH_2^{2+}$ ($[HNO_2]_0 = 1.667 \times 10^{-3}$ M, $[FDSH_2^{2+}]_0 = 1.667 \times 10^{-2}$ M, $[HClO_4]_0 = 0.15$ M, ionic strength ($NaClO_4$) = 1.00 M, λ = 370 nm, 25.0 °C). Solid line for the data fitted to autocatalytic equation.

at the beginning of reaction, respectively, we obtain the following expression:

$$A_t = A_\infty + \frac{\varepsilon' k_3 (A_0 - A_\infty)}{[\varepsilon' k_3 - 5/6k_2(A_0 - A_\infty)]e^{k_3 t} + 5/6k_2(A_0 - A_\infty)} \quad (10)$$

where $\varepsilon' = 43.65$ mol^{-1} dm^3 for cells with a 1 cm path length.

The typical behavior of a kinetic run is shown in Fig. 1 and the z-shape of the absorbance *vs.* time plot is clearly observed. The solid line in the figure shows the good fit of the experimental data to eqn (10) and results are reported in Table 1.

Since $k_3 = k_1 + 5/6k_2[HNO_2]_0 = (k_{NO^+}K_{NO^+}K_a^I + 5/6k_{NOSCN}K_{NOSCN}K_a^I[HNO_2]_0)[FDSH_2^{2+}]_0$, if we plot $k_3/[FDSH_2^{2+}]_0$ *vs.* $[HNO_2]_0$, as shown in Fig. 2, a linear dependence is observed where $k_{NO^+}K_{NO^+}K_a^I = (1.1 \pm 0.2) \times 10^{-2}$ M^{-1} s^{-1} and $5/6k_{NOSCN}K_{NOSCN}K_a^I = 17.8 \pm 0.8$ M^{-2} s^{-1}. A linear relationship between $5/6k_2$ and $[FDSH_2^{2+}]_0$ can be seen in Fig. 3, with the slope $5/6k_{NOSCN}K_{NOSCN}K_a^I = 15.4 \pm 0.2$ M^{-2} s^{-1}, a value compatible with that obtained previously. On averaging both results we obtain a value of $5/6k_{NOSCN}K_{NOSCN}K_a^I = 16.6 \pm 1.2$ M^{-2} s^{-1}.

From the intercept and the slope in Fig. 2, and by using previous values for K_{NO^+}, $K_{NO^+} = 3 \times 10^{-7}$ M^{-1}, K_a^I, $K_a^I = 3.24 \times 10^{-6}$ M, and K_{NOSCN}, $K_{NOSCN} = 30$ M^{-2}, we can calculate the values of $k_{NO^+} = (1.1 \pm 0.2) \times 10^{10}$ M^{-1} s^{-1} and $k_{NOSCN} = (2.2 \pm 0.1) \times 10^5$ M^{-1} s^{-1} (see Table 5). The slope in Fig. 3 also allows us to obtain a value of $K_{NOSCN} = (1.90 \pm 0.02) \times 10^5$ M^{-1} s^{-1}.

Table 1 Values of k_3 and $5/6k_2$ obtained from the fit of experimental data to eqn (10) ($[HClO_4]_0 = 0.15$ M, ionic strength ($NaClO_4$) = 1.00 M, 25.0 °C)

$10^3[HNO_2]_0$/M	$10^2[FDSH_2^{2+}]_0$/M	10^3k_3/s^{-1}	$10(5/6k_2)$/M^{-1} s^{-1}
4.49	4.48	4.10 ± 0.04	6.2 ± 0.1
3.58	3.58	2.71 ± 0.01	5.64 ± 0.04
2.67	2.69	1.53 ± 0.01	3.42 ± 0.05
1.36	1.34	0.529 ± 0.004	1.98 ± 0.04
0.711	0.717	0.157 ± 0.002	0.97 ± 0.03

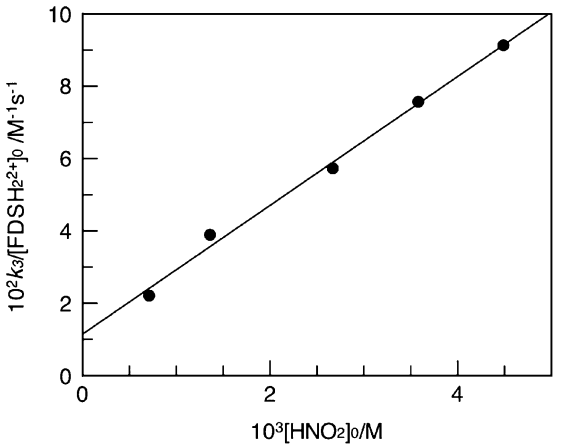

Fig. 2 $k_3/[FDSH_2^{2+}]$ *vs.* $[HNO_2]_0$ ($[HClO_4]_0 = 0.15$ M, ionic strength ($NaClO_4$) = 1.00 M, 25.0 °C).

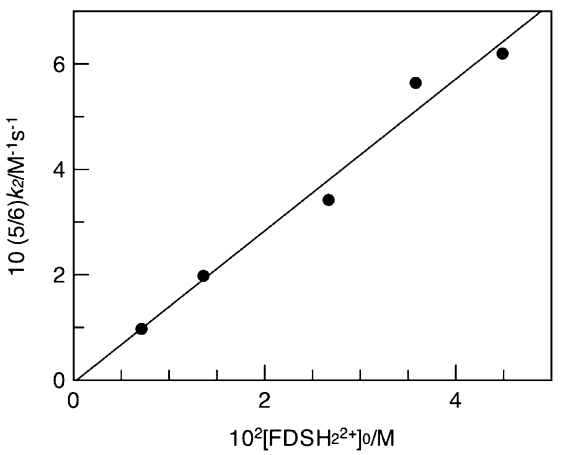

Fig. 3 $5/6k_2$ *vs.* $[FDSH_2^{2+}]$ ($[HNO_2]_0$ ranging from (0.711 to 4.49) × 10^{-3} M, $[HClO_4]_0 = 0.15$ M, ionic strength ($NaClO_4$) = 1.00 M, 25.0 °C).

A set of experiments was performed in which the acid concentration was varied between $[HClO_4] = 8.00 \times 10^{-2}$ and 0.850 M. The results are given in Table 2. The values of $k_3 = (8.9 \pm 0.9) \times 10^{-4}$ s^{-1} and $5/6k_2 = (3.1 \pm 0.4) \times 10^{-1}$ M^{-1} s^{-1} proved to be independent of the acid concentration, supporting the hypothesis that the reaction occurs through the monoprotonated form of the formamidine disulfide. By considering $k_2 = k_{NOSCN}K_{NOSCN}K_a^I[FDSH_2^{2+}]_0$ we can calculate the value of $K_{NOSCN} = (2.3 \pm 0.3) \times 10^5$ M^{-1} s^{-1} and with $k_3 = (k_{NO^+}K_{NO^+}K_a^I + 5/6k_{NOSCN}K_{NOSCN}K_a^I[HNO_2]_0)[FDSH_2^{2+}]_0$ we can obtain $k_{NO^+} = (2.3 \pm 0.2) \times 10^{10}$ M^{-1} s^{-1} (see Table 5).

2. Influence of added SCN^-

The addition of the thiocyanate anion to the reaction medium leads to eqn (6) being rewritten as:

$$r = k_1[HNO_2] + k_{NOSCN}K_{NOSCN}K_a^I[FDSH_2^{2+}]_0[HNO_2] \times\{5/6([HNO_2]_0 - [HNO_2]) + [SCN^-]\} \quad (11)$$

When $[SCN^-]_0 \gg [HNO_2]_0$ eqn (11) is simplified to:

$$r = (k_1 + k_2[SCN^-]_0)[HNO_2] \quad (12)$$

Table 2 Values of k_3 and $5/6k_2$ obtained from the fit of experimental data to eqn (10) ($[HNO_2]_0 = 1.667 \times 10^{-3}$ M, $[FDSH_2^{2+}]_0 = 1.667 \times 10^{-2}$ M, ionic strength ($NaClO_4$) = 1.00 M, 25.0 °C)

$10[HClO_4]_0$/M	$10^4 k_3/s^{-1}$	$10(5/6k_2)/M^{-1}\ s^{-1}$
0.800	7.3 ± 0.1	2.26 ± 0.06
1.70	8.5 ± 0.1	2.95 ± 0.06
2.50	8.8 ± 0.1	3.24 ± 0.08
4.50	9.1 ± 0.1	3.0 ± 0.1
7.00	10.0 ± 0.1	3.6 ± 0.1
8.50	9.9 ± 0.2	3.4 ± 0.1

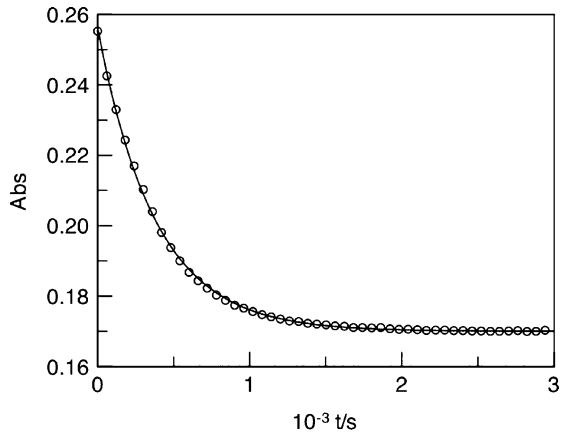

Fig. 4 Absorbance *vs.* time plot for the reaction of HNO_2 (1.667×10^{-3} M) with $FDSH_2^{2+}$ in the presence of SCN^- ($[SCN^-] = 5.50 \times 10^{-3}$ M, $[FDSH_2^{2+}]_0 = 1.667 \times 10^{-2}$ M, $[HClO_4]_0 = 0.15$ M, ionic strength ($NaClO_4$) = 1.00 M, λ = 370 nm, 25.0 °C). Solid line for data fit to a single exponential decay.

which corresponds to a first order rate equation with $k_{obs} = k_1 + k_2[SCN^-]_0$. An absorbance *vs.* time plot for a reaction carried out with added SCN^- is shown in Fig. 4.

The results obtained on varying $[SCN^-]$ are given in Table 3 and, since $k_{obs} = (k_{NO^+}K_{NO^+}K_a^I + k_{NOSCN}K_{NOSCN}K_a^I[SCN^-]_0)[FDSH_2^{2+}]_0$, when plotting $k_{obs}/[FDSH_2^{2+}]_0$ *vs.* $[SCN^-]_{add}$ a linear dependence is observed where the intercept $k_{NO^+}K_{NO^+}K_a^I = (5.4 \pm 0.3) \times 10^{-2}\ M^{-1}\ s^{-1}$ and the slope $k_{NOSCN}K_{NOSCN}K_a^I = 18.5 \pm 0.2\ M^{-2}\ s^{-1}$ (Fig. 5). From the intercept and slope, the values of $k_{NO^+} = (5.6 \pm 0.3) \times 10^{10}\ M^{-1}\ s^{-1}$ and $k_{NOSCN} = (1.91 \pm 0.02) \times 10^5\ M^{-1}\ s^{-1}$ (see Table 5) can be calculated.

3. Influence of added Br^- and Cl^-

When a halide anion X^- is present in the reaction medium a new contribution to the rate must be added to eqn (12). If a nucleophile such as Br^- or Cl^- is added to the reaction medium a new pathway leading to SCN^- is opened up. On the other hand, when halide anions are added to the reaction they compete with the thiocyanate for the nitrous acid in order to produce the nitrosyl halide. In this struggle for the nitrous acid two conflicting effects are balanced. On the one hand the equilibrium constants ($K_{NOSCN} \gg K_{NOX}$) and on the other the concentration of the nucleophilic species $[X^-] \gg [SCN^-]$. From this balance we would expect to observe autocatalytic behavior at low concentrations of X^- and when the difference between the equilibrium constants is greater. In the presence of halides the situation should be represented as:

$$r = k_1[HNO_2] + k_2(5/6([HNO_2]_0 - [HNO_2]))[HNO_2] + k_4[HNO_2] \quad (13)$$

where $k_4 = k_{NOX}K_{NOX}K_a^I[FDSH_2^{2+}]_0[X^-]_0$.

From the analysis of eqn (13) it can easily be seen that when $k_2(5/6([HNO_2]_0 - [HNO_2])) \ll k_4$ then the equation can be simplified to:

$$r = (k_1 + k_4)[HNO_2] \quad (14)$$

Integration of the latter equation leads to a single exponential decay.

When the autocatalytic contribution of the non-halide-catalyzed pathway is not depreciable, integration of (13) gives an expression formally equivalent to eqn (9) where $k_5 = (k_1 + k_2(5/6[HNO_2]_0) + k_4)$.

$$[HNO_2] = \frac{k_5[HNO_2]_0}{(k_5 - 5/6k_2[HNO_2]_0)e^{k_3 t} + 5/6k_2[HNO_2]_0} \quad (15)$$

When the influence of the bromide anion was studied with $[Br^-]$ ranging from 1.2×10^{-2} to 0.30 M the absorbance *vs.* time plot exhibited an autocatalytic shape at the lower concentration and first-order behavior for all other concentration values. The resulting pseudo-first-order rate constants k_{obs} are listed in Table 3. From the plot of $k_{obs}/[FDSH_2^{2+}]_0$ *vs.* $[Br^-]$ (Fig. 5), the intercept $k_{NO^+}K_{NO^+}K_a^I = (4.7 \pm 0.6) \times 10^{-2}\ M^{-1}\ s^{-1}$ and the slope $k_{NOBr}K_{NOBr}K_a^I = 1.55 \pm 0.03\ M^{-2}\ s^{-1}$ allow us to obtain the nitrosation rate constants by NO^+, $k_{NO^+} = (4.7 \pm 0.6) \times 10^{10}\ M^{-1}\ s^{-1}$, and NOBr, $k_{NOBr} = (9.4 \pm 0.2) \times 10^6\ M^{-1}\ s^{-1}$ (see Table 5) from the slope (Fig. 5).

Experiments carried out at the lower chloride anion concentrations ($[Cl^-] \leq 0.23$ M) showed a z-shaped absorbance *vs.* time plot, which indicates an appreciable contribution from the autocatalytic pathway. The kinetic data for this set of experiments were fitted to eqn (15) and the resulting values for k_5 and $5/6k_2$ are listed in Table 4.

As predicted by the kinetic model, k_2 was invariant with $[Cl^-]$ and the mean value for $5/6k_2$ is $(2.9 \pm 0.2) \times 10^{-1}\ M^{-1}\ s^{-1}$. On using this value the bimolecular rate constant k_{NOSCN} was calculated, $k_{NOSCN} = (2.1 \pm 0.1) \times 10^5\ M^{-1}\ s^{-1}$, and this is in very good agreement with previously obtained values. Since $k_5/[FDSH_2^{2+}]_0 = \{k_{NO^+}K_{NO^+}K_a^I + k_{NOSCN}K_{NOSCN}K_a^I(5/6[HNO_2]_0)\} + k_{NOCl}K_{NOCl}K_a^I[Cl^-]_0$, then from the plot $k_5/[FDSH_2^{2+}]$ *vs.* $[Cl^-]_0$ (see Fig. 6), we obtain an intercept, $\{k_{NO^+}K_{NO^+}K_a^I + k_{NOSCN}K_{NOSCN}K_a^I(5/6[HNO_2]_0)\} = (5.4 \pm 0.1) \times 10^{-2}\ M^{-1}\ s^{-1}$, and a slope, $k_{NOCl}K_{NOCl}K_a^I = (1.5 \pm 0.2) \times 10^{-1}\ M^{-2}\ s^{-1}$. From the intercept, and on using the previously obtained value of $k_{NOSCN} = (2.1 \pm 0.1) \times 10^5\ M^{-1}\ s^{-1}$, we can calculate k_{NO^+}, $k_{NO^+} = (1.35 \pm 0.02) \times 10^{10}\ M^{-1}\ s^{-1}$ (see Table 5). From the slope we can obtain the bimolecular rate constant for formamidine disulfide nitrosation by NOCl, $k_{NOCl} = (4.2 \pm 0.6) \times 10^7\ M^{-1}\ s^{-1}$ (Table 5).

For higher chloride anion concentrations ($[Cl^-] > 0.4$ M) the kinetics are first order and the data could be fitted to a first exponential decay (Table 3). The intercept of the linear plot $k_{obs}/[FDSH_2^{2+}]_0$ *vs.* $[Cl^-]$ (Fig. 5) has a value of $(3.9 \pm 0.2) \times$

Table 3 Values of k_{obs} obtained from the fit of experimental data to a single exponential decay. ($[FDSH_2^{2+}]_0 = 1.667 \times 10^{-2}$ M, $[HNO_2]_0 = 1.667 \times 10^{-3}$ M, $[HClO_4]_0 = 0.15$ M, Ionic strength ($NaClO_4$) = 1.00 M

$10^2[SCN^-]_{add}$/M	$10^3k_{obs}/s^{-1}$	$10[Br^-]$/M	$10^3k_{obs}/s^{-1}$	$10[Cl^-]$/M	$10^3k_{obs}/s^{-1}$
0.280	1.72 ± 0.02	0.500	2.01 ± 0.01	4.00	1.549 ± 0.005
0.550	2.65 ± 0.02	1.00	3.47 ± 0.02	5.00	1.816 ± 0.004
1.40	5.24 ± 0.05	2.00	5.91 ± 0.08	6.00	2.011 ± 0.009
2.00	6.98 ± 0.05	2.50	7.25 ± 0. 07	6.50	2.133 ± 0.007
2.75	9.4 ± 0.1			7.00	2.24 ± 0.01

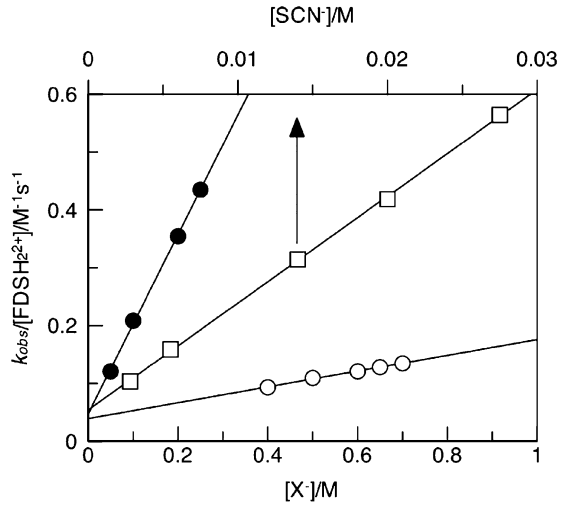

Fig. 5 $k_{obs}/([FDSH_2^{2+}]_0$ *vs.* (○)$[Cl^-]$, (●)$[Br^-]$ and (□)$[SCN^-]$ ($[FDSH_2^{2+}]_0 = 1.667 \times 10^{-2}$ M, $[HNO_2]_0 = 1.667 \times 10^{-3}$ M, $[HClO_4]_0 = 0.15$ M, ionic strength ($NaClO_4$) = 1.00 M, 25.0 °C).

Table 4 Values of k_5 and $5/6k_2$ obtained from the fit of experimental data to eqn (15) ($[HNO_2]_0 = 1.667 \times 10^{-3}$ M, $[FDSH_2^{2+}]_0 = 1.667 \times 10^{-2}$ M, ionic strength ($NaClO_4$) = 1.00 M, 25.0 °C)

$10^2[Cl^-]$/M	$10^3k_5/s^{-1}$	$10(5/6k_2)/M^{-1}\ s^{-1}$
1.70	0.932 ± 0.008	2.97 ± 0.06
3.50	0.964 ± 0.008	2.89 ± 0.05
7.00	1.096 ± 0.008	2.88 ± 0.06
0.130	1.18 ± 0.01	2.46 ± 0.08
0.230	1.49 ± 0.03	3.1 ± 0.2

10^{-2} M^{-1} s^{-1} for $k_{NO^+}K_{NO^+}K_a^I$, which corresponds to k_{NO^+} = (4.0 ± 0.1) × 10^{10} M^{-1} s^{-1}. This value is in good agreement with those obtained from the previous experiments. From the slope we obtain value of $k_{NOCl}K_{NOCl}K_a^I$ = (1.36 ± 0.04) × 10^{-1} M^{-2} s^{-1}. The value of k_{NOCl} = (3.8 ± 0.1) × 10^7 M^{-1} s^{-1}

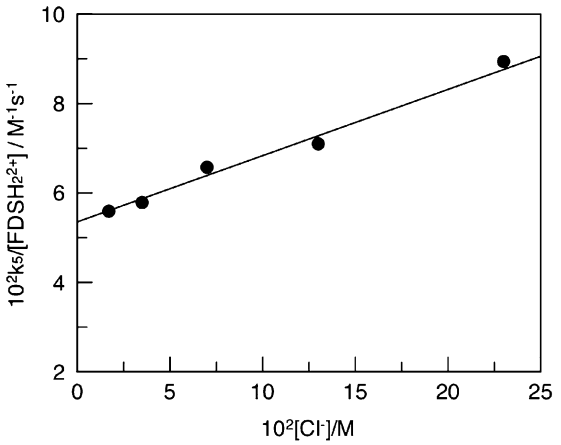

Fig. 6 $k_5/([FDSH_2^{2+}]_0$ *vs.* $[Cl^-]$ ($[FDSH_2^{2+}]_0 = 1.667 \times 10^{-2}$ M, $[HNO_2]_0 = 1.667 \times 10^{-3}$ M, $[HClO_4]_0 = 0.15$ M, ionic strength ($NaClO_4$) = 1.00 M, 25.0 °C).

is similar to that obtained at lower chloride anion concentrations (see Table 5).

4. Reaction mechanism

The mechanism for the formation of N-nitroso compounds depends largely on the functionality of the nitrosating substrate. The mechanisms for the nitrosation of amides and ureas have been widely investigated[36–41] and a large number of differences have been found between nitrosation of these compounds and amines. In the case of amines, the attack of the nitrosating agent on the free amine is rate determining, while for amides and ureas this first step is fast, the slow step being a proton transfer from an intermediate to the reaction medium. In the latter case the reaction seems to occur initially on the oxygen atom, and a fast internal rearrangement leads to the thermodynamically more stable *N*-nitrosoamide. Guanidines can be considered nitrogenated analogs of ureas.

Table 5 Compilation of kinetic parameters obtained under autocatalytic or first-order conditions for FDS nitrosation by NO^+, NOSCN, NOBr and NOCl

Experimental conditions	$k_{NO^+}/M^{-1}\ s^{-1}$	$k_{NOSCN}/M^{-1}\ s^{-1}$	$k_{NOBr}/M^{-1}\ s^{-1}$	$k_{NOCl}/M^{-1}\ s^{-1}$
No added X^-	$(1.1^a \pm 0.2) \times 10^{10}$	$(2.2^a \pm 0.1) \times 10^5$		
	$(2.3^b \pm 0.2) \times 10^{10}$	$(1.90^a \pm 0.02) \times 10^5$		
		$(2.3^b \pm 0.3) \times 10^5$		
Added SCN^-	$(5.6 \pm 0.3) \times 10^{10}$	$(1.91 \pm 0.02) \times 10^5$		
Added Br^-	$(4.7 \pm 0.6) \times 10^{10}$		$(9.4 \pm 0.2) \times 10^6$	
Added Cl^-	$(1.35^c \pm 0.02) \times 10^{10}$	$(2.1^c \pm 0.1) \times 10^5$		$(4.2^c \pm 0.6) \times 10^7$
	$(4.0^d \pm 0.2) \times 10^{10}$			$(3.8^d \pm 0.1) \times 10^7$
Mean values	$(3.2 \pm 1.8) \times 10^{10}$	$(2.1 \pm 0.2) \times 10$	$(9.4 \pm 0.2) \times 10^6$	$(4.0 \pm 0.2) \times 10^7$

[a] Obtained under autocatalytic conditions form the influence of $[FDSH_2^{2+}]_0$. [b] Obtained under autocatalytic conditions from the influence of $[HClO_4]$. [c] Obtained under autocatalytic conditions. [d] Obtained under first order conditions.

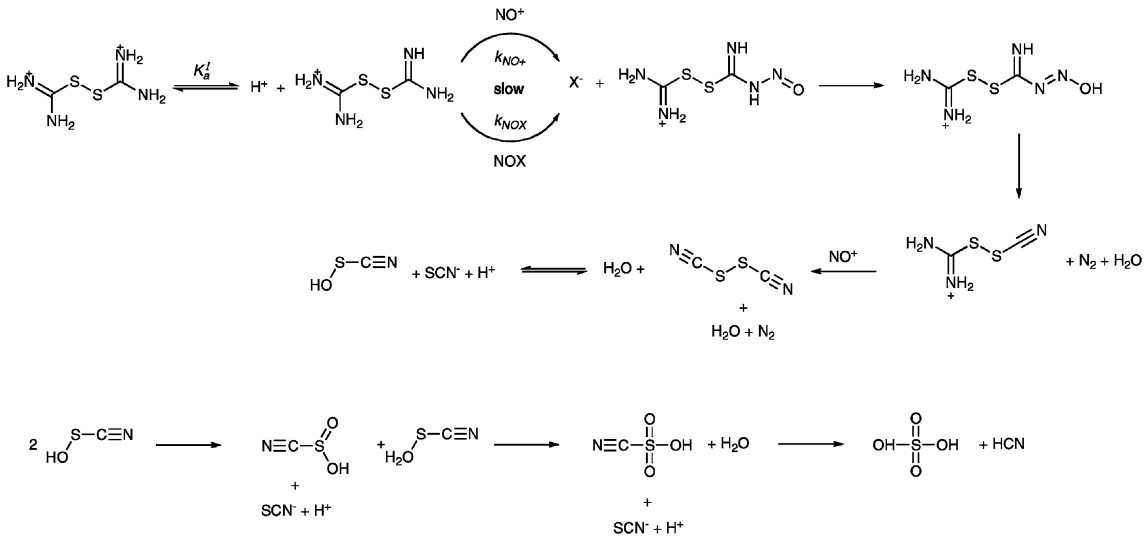

Scheme 3

However, their peculiar structure makes them compounds of great basicity and, in this sense, they are more similar to amines than ureas. Mechanisms for guanidine nitrosation show parallels with that found for ureas.[42–44]

Experimental results obtained in the nitrosation of formamidine disulfide, mainly the existence of halide catalysis, are compatible with the amine nitrosation mechanism, where the attack of the nitrosating agent is the rate limiting step. The values obtained for k_{NO^+}, despite the wide range of values, indicate that the rate of the nitrosation step is diffusion controlled. The broad range in the results arises from the fact that they are obtained from the intercept of a linear plot with a significant error associated. The rate values of catalyzed pathways follow the expected order $SCN^- \ll Br^- < Cl^-$. This kinetic evidence and the formation of molecular nitrogen strongly suggest that the FDS behaves like an amine as far as nitrosation is concerned.

The proposed mechanism is shown in Scheme 3. Attack of the effective nitrosating species on the monoprotonated formamidine disulfide is the rate-limiting step. The resulting *N*-nitrosoformamidine disulfide suffers deamination, in analogy with the process that occurs with primary amines. A second nitrosation/deamination process should take place at the amidine moiety of the amino(cyanodisulfanyl)methaniminium ion, leading to the formation of thiocyanogen $(SCN)_2$. The formation of the thiocyanate ion, sulfuric acid and hydrogen cyanide arise from thiocyanogen hydrolysis according to the findings reported by Bjerrum and Kirschner.[45]

The nitrosation bimolecular rate constants, Table 5, show the expected behavior for the nitrosation of a poorly basic amine. As expected, it can be observed that reactivity decreases in the order $NO^+ > NOCl > NOBr > NOSCN$. This behavior is justified on the basis of the polarity of the X–NO bond. An increase in the electronegativity of X leads to an increase in the positive charge on the nitrogen atom, making the nitroso group a better electrophilic acceptor and therefore increasing the reactivity.[9]

Acknowledgements

This work was supported by Spain's Ministerio de Ciencia y Tecnología (Project CTQ2005-04779), Xunta de Galicia (PGIDIT07-PXIB209041PR and 2007/085) and by the Fundação para a Ciência e Tecnologia-Portugal (PPCDT/QUI/57077/2004). J. A. Moreira acknowledges for the SFRH/BSAB/737/2007 grant.

References

1 P. Rys, in *Advances in Color Chemistry Series, Vol. 4, Physico-Chemical Principles of Color Chemistry*, eds. A. T. Peters and H. S. Freeman, Blackie Academic Press, Glasgow, 1996, p. 1.
2 B. B. Sithole and R. D. Guy, *Sci. Total Environ.*, 1986, **50**, 227.
3 G. da Silva, E. M. Kennedy and B. Z. Dlugogorski, *J. Am. Chem. Soc.*, 2005, **127**, 3664.
4 K. B. Shapiro, J. H. Hotchkiss and D. A. Roe, *Food Chem. Toxicol.*, 1991, **29**, 751.
5 J. M. Barnes and P. N. Magee, *Br. J. Ind. Med.*, 1954, **11**, 167.
6 *Chemical Carcinogens*, ed. C. E. Searle, ACS Monograph 182, American Chemical Society, Washington, DC, 2nd edn, 1985.
7 F. K. Zimmermann, *Biochem. Pharmacol.*, 1971, **20**, 985.
8 H. Druckrey, *Xenobiotica*, 1973, **3**, 271.
9 D. L. H. Williams, *Nitrosation Reactions and the Chemistry of Nitric Oxide*, Elsevier, Amsterdam, 2004.
10 G. Rabai, R. T. Wang and K. Kustin, *Int. J. Chem. Kinet.*, 1993, **25**, 53.
11 W. Wang, M. N. Schuchmann, H.-P. Schuchmann, W. Knolle, J. von Sonntag and C. von Sonntag, *J. Am. Chem. Soc.*, 1999, **121**, 238.
12 P. K. Srivastava, R. D. Sharma and M. Saleem, *Curr. Sci.*, 1976, **45**, 764.
13 J. Li and J. D. Miller, *Hydrometallurgy*, 2002, **63**, 215.
14 J. B. Walker, in *The Enzymes*, ed. P. D. Boyer, Academic Press, NY, 1973, vol. IX, p. 501.
15 A. H. Neims, D. S. Coffey and L. Hellerman, *J. Biol. Chem.*, 1966, **241**, 5491.
16 J. Casado, A. Crasto, J. R. Leis and M. A. Lopez Quintela, *Monatsh. Chem.*, 1983, **114**, 639.
17 J. H. Ridd, *Adv. Phys. Org. Chem.*, 1978, **16**, 1.
18 N. S. Bayliss, R. Dingle, D. W. Watts and R. C. Wilkie, *Aust. J. Chem.*, 1963, **16**, 933.
19 J. H. Ridd, *Q. Rev. Chem. Soc.*, 1961, **15**, 418.
20 H. Schmid and E. Hallaba, *Monatsh. Chem.*, 1956, **87**, 560.
21 E. D. Hughes and J. H. Ridd, *J. Chem. Soc.*, 1958, 82.
22 G. Stedman and P. A. E. Whincup, *J. Chem. Soc.*, 1963, 5796.
23 M. R. Crampton, J. T. Thompson and D. L. H. Williams, *J. Chem. Soc., Perkin Trans. 2*, 1979, 18.
24 J. R. Perrott, G. Stedman and N. Uysal, *J. Chem. Soc., Dalton Trans.*, 1976, 2058.
25 J. R. Park and D. L. H. Williams, *J. Chem. Soc., Perkin Trans. 2*, 1972, 2158.

26 T. A. Meyer and D. L. H. Williams, *J. Chem. Soc., Perkin Trans. 2*, 1981, 361.
27 A. Castro, J. R. Leis and M. E. Peña, *J. Chem. Res. (S)*, 1988, 216.
28 L. Storch, *Monatsh. Chem.*, 1890, **11**, 452.
29 A. E. Werner, *J. Chem. Soc., Trans.*, 1912, **101**, 2166; A. E. Werner, *J. Chem. Soc., Trans.*, 1912, **101**, 2180.
30 M. E. Coade and A. E. Werner, *J. Chem. Soc., Trans.*, 1913, **102**, 1221.
31 K. Y. Al-Mallah, P. Collings and G. Stedman, *J. Chem. Soc., Dalton Trans.*, 1974, 2469.
32 P. Collings, M. S. Garley and G. Stedman, *J. Chem. Soc., Dalton Trans.*, 1981, 331.
33 M. S. Garley, H. Miller and G. Stedman, *J. Chem. Soc., Dalton Trans.*, 1984, 1959.
34 L. Garcia-Rio, C. G. Munkley and G. Stedman, *J. Chem. Soc., Perkin Trans. 2*, 1996, 159.
35 R. J. Leatherbarrow, *GraFit Version 5*, Erithacus Software Ltd, Horley, UK, 2002.
36 G. Hallett and D. L. H. Williams, *J. Chem. Soc., Perkin Trans. 2*, 1980, 1372.
37 A. Castro, E. Iglesias, J. R. Leis, M. E. Peña and J. Vázquez-Tato, *J. Chem. Soc., Perkin Trans. 2*, 1986, 1725.
38 F. Meijide, J. Vázquez-Tato, J. Casado, A. Castro and M. Mosquera, *J. Chem. Soc., Perkin Trans. 2*, 1987, 159.
39 C. Bravo, P. Hervés, J. R. Leis and M. E. Peña, *J. Chem. Soc., Perkin Trans. 2*, 1991, 2091.
40 L. García-Rio, J. R. Leis, J. A. Moreira and F. Norberto, *J. Chem. Soc., Perkin Trans. 2*, 1998, 1613.
41 G. Gonzalez-Alatorre, S. H. Guzmán-Maldonado, E. M. Escamilla-Silva, G. Lorca-Piña and C. Hernández-Benítez, *Int. J. Chem. Kinet.*, 2004, **36**, 273.
42 F. Norberto, J. A. Moreira, E. Rosa, J. Iley, J. R. Leis and M. E. Peña, *J. Chem. Soc., Perkin Trans. 2*, 1993, 1561.
43 J. R. Leis, F. Norberto, J. A. Moreira and J. Iley, *J. Chem. Res. (S)*, 1997, 88.
44 I. Fernández, P. Hervés and M. Parajó, *J. Phys. Org. Chem.*, 2008, **21**, 713.
45 N. Bjerrum and A. Kirschner, *Kgl. Danske Videnskab. Selskab. Math. Fys. Ser. 8*, 1918, **5**, 57; N. Bjerrum and A. Kirschner, *Chem. Abstr.*, 1919, **13**, 1057.

